Lipophilic ternary complexes in liquid–liquid extraction of trivalent lanthanides

Gregg J. Lumetta [a] , Tatiana G. Levitskaia [a] , Stan L. Latesky [b] , Renesha V. Henderson [b] , Emilio A. Edwards [b] , Jenifer C. Braley [a] & Sergey I. Sinkov [a]

[a] Pacific Northwest National Laboratory , PO Box 999, MSIN P7-25, Richland , WA 99352 , USA

[b] College of Science & Mathematics, University of the Virgin Islands , 2 John Brewers Bay Road, St. Thomas, VI 00802 , US Virgin Islands
Published online: 14 Feb 2012.

PLEASE SCROLL DOWN FOR ARTICLE

Taylor & Francis
Taylor & Francis Group

Lipophilic ternary complexes in liquid–liquid extraction of trivalent lanthanides

GREGG J. LUMETTA*†, TATIANA G. LEVITSKAIA†, STAN L. LATESKY‡,
RENESHA V. HENDERSON‡, EMILIO A. EDWARDS‡,
JENIFER C. BRALEY† and SERGEY I. SINKOV†

†Pacific Northwest National Laboratory, PO Box 999,
MSIN P7-25, Richland, WA 99352, USA
‡College of Science & Mathematics, University of the Virgin Islands,
2 John Brewers Bay Road, St. Thomas, VI 00802, US Virgin Islands

The formation of ternary complexes between lanthanide ions [Nd(III) or Eu(III)], octyl(phenyl)-*N*,*N*-diisobutyl-carbamoylmethylphosphine oxide (CMPO), and bis-(2-ethylhexyl)phosphoric acid (HDEHP) was probed by liquid–liquid extraction and spectroscopic techniques. Equilibrium modeling of data for the extraction of Nd(III) or Eu(III) from lactic acid media into *n*-dodecane solutions of CMPO and HDEHP indicates the predominant extracted species are of the type $[Ln(AHA)_2(A)]$ and $[Ln(CMPO)(AHA)_2(A)]$, where $Ln = Nd$ or Eu and A represents the $DEHP^-$ anion. FTIR (for both Eu and Nd) and visible spectrophotometry (in the case of Nd) indicate the formation of the $[Ln(CMPO)(A)_3]$ complexes when CMPO is added to *n*-dodecane solutions of the LnA_3 compounds. Both techniques indicate a stronger propensity of CMPO to complex Nd(III) *versus* Eu(III).

Keywords: Lanthanide separation; Actinide separation; Lanthanide/actinide separation; CMPO; HDEHP

1. Introduction

The concept of synergism is well-established in liquid–liquid extraction chemistry [1–4]. Synergism can be defined as "the co-operative effect of two (or more) extractants where the distribution ratio for the combination is greater than the largest individual distribution ratio (measured under comparable conditions)" [5]. Liquid–liquid extraction systems combining different extractants have recently been investigated for separating trivalent lanthanides from trivalent actinides [6]. Understanding and controlling the synergic interactions of the combined extractants is critical to developing effective separation systems. One such liquid–liquid extraction system combines octyl(phenyl)-*N*,*N*-diisobutyl-carbamoylmethylphosphine oxide (CMPO) and bis-(2-ethylhexyl)phosphoric acid (HDEHP) into a single process solvent for separating
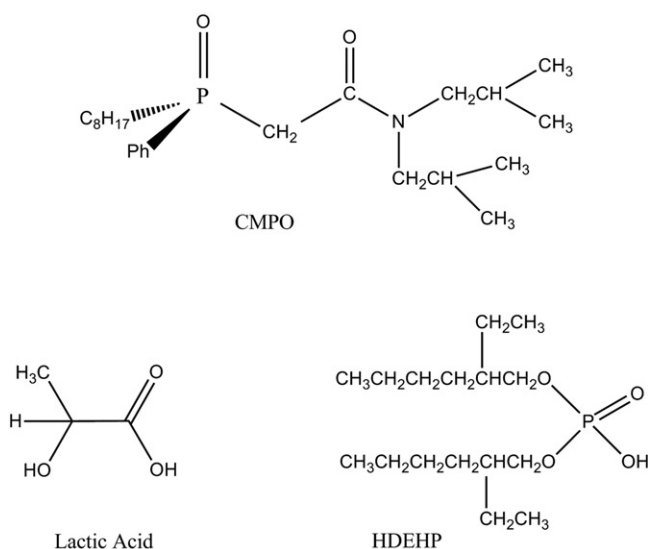

Figure 1.   Chemical structures of the extractants CMPO and HDEHP, and of lactic acid.

trivalent actinides (i.e., Am and Cm) from the lanthanides [7, 8]. Figure 1 provides the chemical structures of CMPO and HDEHP.

In the combined CMPO/HDEHP liquid–liquid extraction system, the trivalent actinides and lanthanides are co-extracted from nitric acid media. In this regard, the system is akin to the transuranic extraction (TRUEX) process [9]. Contacting the loaded solvent containing the lanthanides and actinides with a carboxylate-buffered solution of diethylenetriaminepentaacetic acid at pH $\sim$3.5 results in selective transfer of the actinides into the aqueous phase, thus separating them from the lanthanides. Under these conditions, the process is akin to the trivalent actinide-lanthanide separations by phosphorus-reagent extraction from aqueous complexes (TALSPEAK) process [10]. However, we have shown that there are some differences in the trends in the lanthanide/ Am separation factors in the combined CMPO/HDEHP system compared to those in the TALSPEAK system (which utilizes only HDEHP as extractant) [8]. Specifically, in the case of TALSPEAK, the poorest separation factor is observed for the Nd/Am couple, whereas in the combined CMPO/HDEHP system the poorest separation factor is observed for the Sm/Am couple. It was hypothesized that these differences are manifestations of differences in the magnitudes of the synergic extractions of the lanthanides. Furthermore, the extraction of Am(III) and Eu(III) with CMPO from $\geq$1 mol L^{-1} HNO$_3$ is suppressed by the addition of HDEHP (compared to the TRUEX process), suggesting that the two extractant compounds might not behave independently in the organic phase.

To gain further insight into the underlying chemistry of the combined CMPO/ HDEHP liquid–liquid extraction system we undertook a series of studies to (1) determine the likely extraction equilibria for extraction of Nd(III) and Eu(III) from lactic acid media, and (2) spectroscopically determine the complexation constants for binding of CMPO to Nd(III) and Eu(III) in the fully loaded Ln/HDEHP/*n*-dodecane system. The results of this study are reported herein.

2. Experimental

2.1. *Materials*

CMPO was procured from Strem Chemicals, Inc. (Newburyport, MA) and was purified as previously described [8]. HDEHP was obtained from Aldrich (Milwaukee, WI). The HDEHP was purified according to the method reported in the literature [11]. Normal dodecane, $NdCl_3 \cdot xH_2O$ ($x = 5$ or 6), and $EuCl_3 \cdot 6H_2O$ were obtained from Alfa Aesar (Ward Hill, MA) and used as-received.

2.2. *Distribution measurements*

A $3.3 \, mol \, L^{-1}$ stock solution of DL-lactic acid was boiled for 24 h to convert the oligomeric fraction to monomeric lactic acid [12] and was then standardized by potentiometric titration with NaOH. The $3.3 \, mol \, L^{-1}$ lactic acid solution (22.73 mL) was mixed with the desired amount of $NdCl_3$ or $EuCl_3$ and 6.0 mL of $1.06 \, mol \, L^{-1}$ HCl was added for pH adjustment. The resulting solution was diluted to 50 mL with deionized water. The Nd concentration in the resulting solution was $1.75 \times 10^{-4} \, mol \, L^{-1}$ or $1.79 \times 10^{-4} \, mol \, L^{-1}$, depending on the particular preparation. The corresponding Eu solution contained $1.95 \times 10^{-4} \, mol \, L^{-1}$ Eu. The pH was 1.0 for these solutions. The organic extractant solutions were prepared by mixing stock *n*-dodecane solutions of HDEHP and CMPO in the desired molar ratios and diluting to the required volume with *n*-dodecane.

Equal volumes of the aqueous and organic phases were mixed using either a wrist-action shaker or a vortex mixer for a minimum of 1 h. Selected measurements were made at longer contact times to verify equilibrium had been obtained after 1 h. After the designated equilibration time, the two phases were separated by centrifugation. In the case of the Eu extractions, the solutions were spiked with [155]Eu (Isotope Products Laboratory, Valencia, CA) before initiating mixing. After equilibration, samples were taken from each phase and the relative [155]Eu activity in each sample was determined using a Packard Cobra II Auto-Gamma counter. For the Nd extractions, the organic phase was removed after equilibration and an aliquot of the aqueous phase was taken for analysis. The Nd concentrations in the initial and final aqueous phases were determined by inductively coupled plasma optical emission spectroscopy (ICP-OES). The organic-phase Nd concentration was calculated by difference.

2.3. *SXLSQI modeling of the extraction data*

Values of the Nd or Eu distribution ratio (D_{Ln}) were used as input to the solvent extraction modeling program SXLSQI [13]. Nonideality effects were taken into account by using Pitzer parameters for aqueous ions [14], the Hildebrand–Scott treatment for nonionic effects in the organic phase [15], and the Debye–Hückel treatment for electrostatic effects in the organic phase [14]; all the calculated extraction constants are thus corrected to infinite dilution. The program converts the molar concentration to the molality scale employed in the Pitzer treatment using Masson coefficients [16]. The solubility parameters and molar volumes of the extractants were estimated from group contributions [15] or refined during modeling. Table 1 summarizes the

Table 1. Nonideality parameters used in SXLSQI modeling of the Nd and Eu extraction data.

| Ion | Masson coefficients[a] | | |
	V_0 (cm^3 mol^{-1})	S_V (cm^3 L$^{1/2}$ mol$^{-3/2}$)	Source
Nd^{3+}	21.34	1.91	[16]
Na$^+$	−1.2	1.2	
Cl$^-$	17.8	0.95	
Lac$^-$	47	3.42	Value for acetate was used [16]

| Interaction | Pitzer parameters | | | | |
	$\beta^{(0)}$	$\beta^{(1)}$	$C\phi$	α	
Na$^+$ – Cl$^-$	0.0765	0.2664	0.00127	2.0	[14]
Na$^+$ – Lac$^-$	0.10875	0.3655	−0.00188	2.0	[27]
H$^+$ – Cl$^-$	0.1775	0.2945	0.0008	2.0	[14]
H$^+$ – Lac$^-$	−0.01797	1.1616	0.02263	2.0	[27]
	$3/2\beta^{(0)}$	$3/2\beta^{(1)}$	$(3/2)^{3/2}C\phi$	α	
Nd^{3+} – Cl$^-$	0.878	8.40	−0.049	2.0	[14]
Nd^{3+} – Lac$^-$	−0.1119	0.2664	0	2.0	Values for Nd^{3+} – NO$_3^-$ were used [14]

| Species | Other parameters | | |
	V_0[b] (cm^3 mol^{-1})	δ[c] (J$^{1/2}$ cm$^{-3/2}$)	Source
Dodecane	228.6	16.1	[15]
HDEHP (HA)	325.2	18.1	Calculated by group contribution method as described in [15]
CMPO	413.2	21.6	
CMPO · HA	738.4	20.1	
NdA$_3$(HA)$_2$		16.3 ± 0.2	This work. Refined
Nd(CMPO)A$_3$(HA)$_2$		15.1 ± 0.6	This work. Refined
EuA$_3$(HA)$_2$		15.1 ± 0.6	This work. Refined
Eu(CMPO)A$_3$(HA)$_2$		16.3 ± 0.7	This work. Refined

[a]Masson coefficients allow the aqueous density to be estimated for molality–molarity interconversions.
[b]Molar volume of the species in the organic phase.
[c]Hildebrand solubility parameters.

parameters used in the SXLSQI modeling of the extraction data. The goodness of fit for a particular model to the given data set is quantified by the *agreement factor* σ, defined according to the least-squares criterion as $\sigma = [\Sigma w_i(Y_i - Y_{c,i})^2/(N_o - N_p)]^{1/2}$ where Y_i is the *i*th experimentally observed quantity (i.e., D_{Ln}), $Y_{c,i}$ is the corresponding quantity calculated from the model being tested, w_i is the weighting factor defined as the reciprocal of the square of the estimated uncertainty of Y_i, N_o is the number of observations, and N_p is the number of adjustable parameters (i.e., log K values). The value of σ will approach unity when the error of fitting is equal to the estimated experimental error; values less than unity are interpreted as cases of experimental precision being better than the estimated precision.

In this work, the observed values of D_{Ln} and corresponding standard deviation values obtained based on the replicate (3–9) measurements were used as the data input to the

model. In the SXLSQI modeling, logarithmic values of the Ln(III) extraction constants for extraction by HDEHP, with and without CMPO present, were refined simultaneously.

2.4. *Ln–HDEHP–CMPO spectroscopic studies*

Stock solutions of Ln(DEHP)$_3$ (Ln = Nd or Eu) were prepared by repeatedly contacting 0.5 mol L^{-1} HDEHP in *n*-dodecane with aqueous LnCl$_3$ solution until a precipitate was observed at the interface. Based on literature reports, it was assumed that all the extracted Nd or Eu existed in solution as Ln(DEHP)$_3$ under these highly loaded conditions [17]. The Nd and Eu concentrations in these organic-phase solutions were determined by repeatedly contacting a portion of the loaded solvent with 3 mol L^{-1} HNO$_3$, combining the aqueous back-extraction phases, and analyzing for Nd or Eu using ICP-OES. A portion of the depleted solvent phase of known mass was placed in a vacuum oven at 50°C for several days to remove the *n*-dodecane, and then the mass of the remaining HDEHP was determined. The concentrations of Ln(DEHP)$_3$ and total HDEHP could be determined in this way.

Portions of the stock Ln(DEHP)$_3$ solutions were mixed with aliquots of a stock solution of CMPO in *n*-dodecane, and the volume was adjusted with *n*-dodecane such that the total Ln(DEHP)$_3$ concentration in each solution was constant. The Fourier-transform infrared (FTIR) and the visible (Vis) (in the case of Nd) spectra were recorded as quickly as reasonably possible after making up each solution because the Ln(DEHP)$_3$ solutions were unstable with respect to precipitation. FTIR spectra were obtained using a Bruker Alpha FTIR spectrometer at a resolution of 2 cm^{-1}. Transmission spectra were obtained using a liquid IR cell with NaCl windows and a 0.025 mm path length. Spectra consisting of a minimum of 16 averaged acquisitions were obtained against an air background. Vis absorbance spectra were obtained using a Spectronics, Inc. charge-coupled-device ultraviolet-Vis spectrometer. Four spectra for each sample were recorded using a quartz microcell (10-mm path length) and averaged together.

The spectral data were analyzed using HypSpec (Protonic Software, Leeds, UK) [18]. Before input into the HypSpec program, the spectral baselines were corrected using GRAMS/AI^{TM} spectroscopy software (Thermo Galactic, Salem, NH, USA) and the spectrum for *n*-dodecane was subtracted. For the FTIR spectra, the baselines were adjusted to zero at 810, 1325, 1550, and 1750 cm^{-1}. For the Vis spectra (Nd only), the baselines were adjusted to zero at 550 and 620 nm. During the HypSpec modeling, the FTIR data in the range 810–1750 cm^{-1} were analyzed, but the region 1325–1550 cm^{-1} was excluded because of complications in this region from bands attributed to *n*-dodecane. The Nd Vis spectroscopic data were analyzed in the region 550–620 nm.

3. Results

3.1. *Extraction of Nd(III) and Eu(III)*

The distribution ratios for the extraction of Nd(III) and Eu(III) from 1.5 mol L^{-1} lactic acid at pH 1 by HDEHP in *n*-dodecane are presented in figure 2(a) as functions of the initial HDEHP concentration. Based on the mean experimental values, the slopes of the log *D versus* log[*HDEHP*] plots are 2.0 and 2.1 for Nd(III) and Eu(III), respectively.
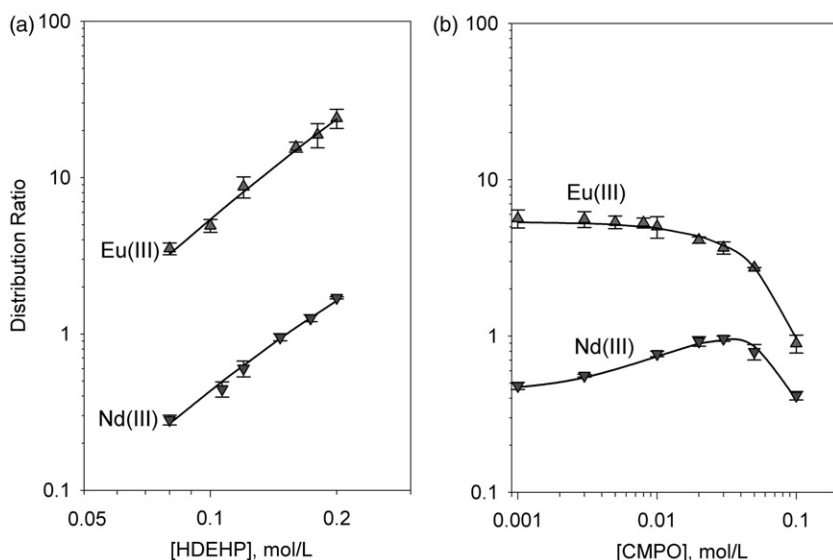
Figure 2. Extraction of Nd(III) and Eu(III) from $1.5\,\mathrm{mol\,L^{-1}}$ lactic acid at pH = 1.0 by (a) variable concentrations of HDEHP in *n*-dodecane and (b) variable concentrations of CMPO in $0.1\,\mathrm{mol\,L^{-1}}$ HDEHP/ *n*-dodecane. All data points were obtained in at least duplicate; in some cases, up to nine measurements were made. Only the mean values are shown on the plot. The solid lines are calculated values based on the model described in the text.
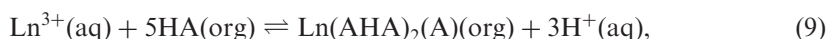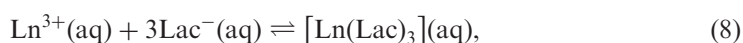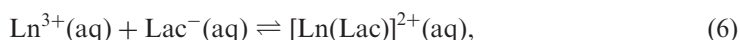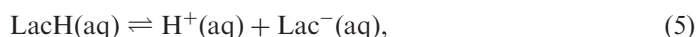
These slope values are lower than those typically reported for extraction of Ln ions from mineral acids with HDEHP, for which slopes of 2.5–3.0 are typically observed [19–22]. Applying simple slope analysis methods to these data would lead to the conclusion that the stoichiometry of the extracted Nd(III) or Eu(III) complex is different from the commonly accepted $[\mathrm{Ln(DEHP \cdot HDEHP)_3}]$ formulation [23]. For this reason, an equilibrium thermodynamic model (using SXLSQI) [13] was applied in interpreting the data. The data in figure 2(a) were combined with the Nd(III) and Eu(III) distribution data obtained as a function of the CMPO concentration (figure 2b) and both data sets were modeled together using SXLSQI as discussed below.

Figure 2(b) presents the Nd(III) and Eu(III) distribution ratios for their extraction from $1.5\,\mathrm{mol\,L^{-1}}$ lactic acid solutions at pH = 1 into $0.1\,\mathrm{mol\,L^{-1}}$ HDEHP/*n*-dodecane with variable concentrations of CMPO. The dependence of D_{Nd} on the CMPO concentration is quite different from that of D_{Eu}. For the Eu(III) distribution data, the general trend is a gradual decrease in D_{Eu} between 0.001 and $0.01\,\mathrm{mol\,L^{-1}}$ CMPO followed by a sharp decrease in D_{Eu} above $0.01\,\mathrm{mol\,L^{-1}}$ CMPO. On the other hand, D_{Nd} increases with increasing CMPO concentration up to $\sim 0.03\,\mathrm{mol\,L^{-1}}$ CMPO, then the D_{Nd} values sharply decrease at higher CMPO concentration. This pattern is very similar to that observed for the extraction of Am(III) with mixtures of HDEHP and tributyl phosphate (TBP) [24]. In the latter case, the TBP dependence of D_{Am} was explained in terms of the following equilibria:

$$\mathrm{Am^{3+}(aq) + 3(HA)_2(org) + L(org) \rightleftharpoons Am(AHA)_3 \cdot L(org) + 3H^+(aq)}, \quad (1)$$

$$\mathrm{(HA)_2(org) + L(org) \rightleftharpoons (HA)_2L(org)}, \quad (2)$$

where HA = HDEHP and L = TBP. At relatively low TBP concentrations, reaction (1) is responsible for the synergic extraction of Am(III) by HDEHP and TBP. However, as the TBP concentration is increased, reaction (2) reduces the effective HDEHP concentration, leading to a decrease in the D_{Am} values. A similar explanation can be invoked for the Nd(III)–HDEHP–CMPO system.

The best SXLSQI fits to the Nd(III) and Eu(III) extraction data shown in figure 2 were obtained by including the following equilibrium reactions:

$$2HA(org) \rightleftharpoons (HA)_2(org), \tag{3}$$

$$CMPO(org) + HA(org) \rightleftharpoons CMPO \cdot HA(org), \tag{4}$$

$$LacH(aq) \rightleftharpoons H^+(aq) + Lac^-(aq), \tag{5}$$

$$Ln^{3+}(aq) + Lac^-(aq) \rightleftharpoons [Ln(Lac)]^{2+}(aq), \tag{6}$$

$$Ln^{3+}(aq) + 2Lac^-(aq) \rightleftharpoons \left[Ln(Lac)_2\right]^+(aq), \tag{7}$$

$$Ln^{3+}(aq) + 3Lac^-(aq) \rightleftharpoons \left[Ln(Lac)_3\right](aq), \tag{8}$$

$$Ln^{3+}(aq) + 5HA(org) \rightleftharpoons Ln(AHA)_2(A)(org) + 3H^+(aq), \tag{9}$$

$$Ln^{3+}(aq) + CMPO + 5HA(org) \rightleftharpoons Ln(CMPO)(AHA)_2(A)(org) + 3H^+(aq), \tag{10}$$

where Lac = CH$_3$CH(OH)COO. The equilibrium constants for reactions (3)–(8) were held constant during refinement of the model. The experimental conditions used to measure the distribution ratios ensured low loading of the organic phase with the lanthanide ion so that Ln^{3+}/HDEHP organic product species used in the SXLSQI modeling could be based on the equilibrium reaction (9), consistent with previously reported speciation analyses [19–21]. It should be noted that the 1 : 1 : 5 stoichiometry of the Ln(CMPO)A$_3$(HA)$_2$ (reaction (10)) product species is only speculatively proposed, and further mechanistic studies are needed to elucidate the exact composition of the Ln–CMPO–HDEHP mixed complex species. The HDEHP dimerization constant for reaction (3) (log K_{dim} = 4.43) was taken from the literature [25]. The equilibrium constant for reaction 4 (logK_4 = 3.07) was previously determined by our group using ^{31}P nuclear magnetic resonance spectroscopy [26]. The acid dissociation constant pK_a for lactic acid was determined by our group to be 3.58 [27]. Reactions (6)–(8) were included in the model with log K_6 = 2.45, log K_7 = 4.39, and log K_8 = 5.44 for Nd(III) [28], and log K_6 = 2.53, log K_7 = 4.60, and log K_8 = 5.88 for Eu(III) [29].

Table 2 presents the refined equilibrium constants for reactions (9) and (10) for both Nd(III) and Eu(III). The calculated values for D_{Nd} and D_{Eu} are plotted as the solid black lines in figure 2. Excellent agreement between the experimental and calculated values was obtained with the model represented by equations (3)–(10). As one would expect for the higher charge density of Eu(III) compared to that of Nd(III), the complexation by HDEHP (reaction (9)) is an order of magnitude stronger for Eu(III) than for Nd(III). This is reflected in the higher Eu(III) distribution ratios. On the other hand, the interaction of CMPO (reaction 10) with Eu(III) is somewhat weaker than that

Table 2.   Equilibrium constants for reactions (9) and (10) for extraction of Nd(III) and Eu(III) from $1.5\,mol\,L^{-1}$ lactic acid solution at pH = 1.0.

	$\log K_9$[a]	$\log K_{10}$[b]	σ
Nd(III)	12.27 ± 0.04	14.73 ± 0.03	1.1
Eu(III)	13.36 ± 0.03	15.00 ± 0.10	0.90

[a]Equilibrium constant for reaction (9).
[b]Equilibrium constant for reaction (10).

with Nd(III). This is indicated by the smaller difference between the $\log K_9$ and $\log K_{10}$ values for Eu(III) [$\log K_{10} - \log K_9 = 1.64$] compared to Nd(III) [$\log K_{10} - \log K_9 = 2.46$]. The relatively weak interaction of Eu(III) with CMPO explains the flat dependence of D_{Eu} *versus* the CMPO concentration up to $0.01\,mol\,L^{-1}$ CMPO, whereas the stronger CMPO complexation to Nd(III) explains the initial rise in D_{Nd} as the CMPO concentration is increased. In both cases, reaction (4) causes the D values to decline rapidly at CMPO concentrations above $0.03\,mol\,L^{-1}$, which is attributed to a decrease in the effective HDEHP concentration as HDEHP is consumed by complexation to CMPO.

3.2. *Spectroscopic investigation of Ln/HDEHP/CMPO systems*

The Nd(III)–HDEHP–CMPO and Eu(III)–HDEHP–CMPO systems were investigated spectroscopically at high HDEHP loading. In the case of the Nd system, the Nd(III) concentration in the fully loaded organic phase was $0.0740\,mol\,L^{-1}$ and the total HDEHP concentration was $0.2655\,mol\,L^{-1}$. Assuming the complex stoichiometry to be Nd(DEHP)$_3$, 16% of the HDEHP remained uncomplexed in the loaded solvent ($0.0435\,mol\,L^{-1}$ uncomplexed HDEHP). The Nd-loaded HDEHP solution was titrated with CMPO up to an approximately 4-molar excess of CMPO relative to Nd(III); 16 incremental additions of CMPO were made. Figure 3(a) illustrates the changes in the ν(C=O) region of the FTIR spectrum for selected conditions upon addition of CMPO to the Nd(DEHP)$_3$ solution. Also shown in the figure are the spectra for CMPO and for a 1:1 mixture of CMPO and HDEHP (predominantly the CMPO·HDEHP adduct, equation (4)). Upon formation of the CMPO·HDEHP adduct, the ν(C=O) band shifts from $1643\,cm^{-1}$ to $1636\,cm^{-1}$. As CMPO is added to the Nd(DEHP)$_3$ solution, two bands become evident in the ν(C=O) region. One band is located at $1638\,cm^{-1}$ and is assigned to the CMPO·HDEHP adduct. The other band is located at $1598\,cm^{-1}$. This latter ν(C=O) band at lower energy can be attributed to the formation of a Nd(DEHP)$_3$·CMPO complex, with the carbonyl oxygen of CMPO involved in the binding.

Figure 3(b) shows the phosphorus–oxygen stretching region in the FTIR spectrum for the Nd(III)–HDEHP–CMPO system. The position of the main P–O–C band of HDEHP shifts little upon complexation to either CMPO or Nd, remaining at approximately $1035\,cm^{-1}$. More significant shifts are observed for the HDEHP ν(P=O) band. The latter band for the HDEHP dimer in *n*-dodecane solution occurs at $1231\,cm^{-1}$. Upon loading with Nd(III), the ν(P=O) band shifts to $1204\,cm^{-1}$, although a shoulder remains on the higher energy range of this band that can be attributed to the uncomplexed HDEHP. Addition of CMPO to the Nd(DEHP)$_3$ complex shifts the
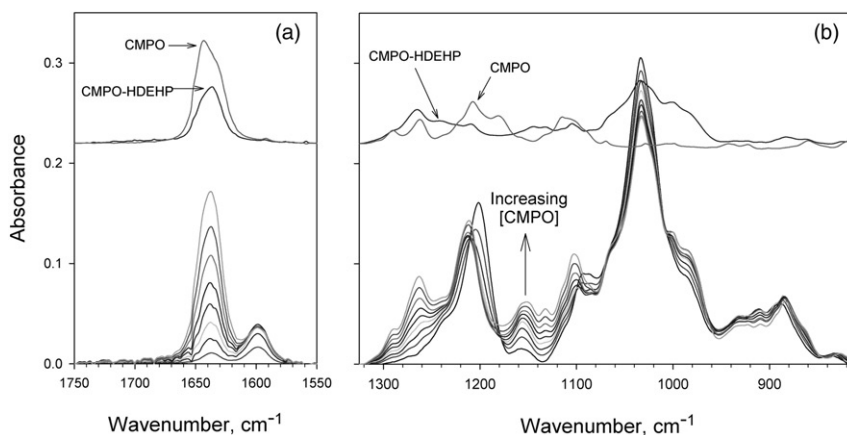
Figure 3. FTIR spectra of $0.0296\,\mathrm{mol\,L^{-1}}$ Nd(DEHP)$_3$ solutions in *n*-dodecane with variable quantities of CMPO added; (a) carbonyl region and (b) phosphoryl region; only a portion of the spectra collected are shown.
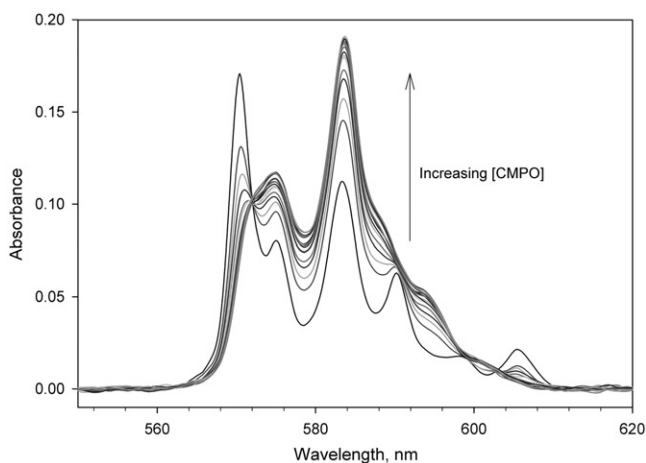

Figure 4. Visible spectra of $0.0296\,\mathrm{mol\,L^{-1}}$ Nd(DEHP)$_3$ solutions in *n*-dodecane with variable quantities of CMPO added.

ν(P=O) band to $1211\,\mathrm{cm^{-1}}$. Again, this is consistent with binding of CMPO to the Nd(III) center, leading to a slight weakening of the Nd–DEHP bond and a corresponding increase in the P=O bond strength. As was the case in the carbonyl region of the FTIR spectrum, bands associated with the CMPO·HDEHP adduct (e.g., 1263 and $1000\,\mathrm{cm^{-1}}$) become increasingly evident as the CMPO concentration is increased. In addition, a band at $1151\,\mathrm{cm^{-1}}$ grows into the FTIR spectrum with increasing CMPO concentration. This latter band can be assigned to the CMPO ν(P=O) band that is shifted upon complexation to the Nd metal center. Ingrowth of the band at $1290\,\mathrm{cm^{-1}}$ suggests the presence of some free CMPO in the system.

Figure 4 shows the changes in the Nd(III) hypersensitive band for the *n*-dodecane solutions of Nd(DEHP)$_3$ as the CMPO concentration is increased. Upon addition of CMPO, the band at 570 nm decreases in intensity relative to the band at 575 nm.

Table 3. Equilibrium constants for reaction (11) for complexation of Ln(DEHP)$_3$ complexes by CMPO.

	Log K_{11}[a]	Log K_{11}[b]
Nd(III)	2.58 ± 0.01	2.98 ± 0.02
Eu(III)	1.01 ± 0.03	Not applicable

[a]Determined by FTIR.
[b]Determined by Vis spectrophotometry.

Concurrently, the band at 583 nm increases in intensity. An isosbestic point is observed at 572 nm, suggesting predominantly two Nd-containing species are present in this chemical system.

The FTIR and Vis spectroscopic data for the Nd(III)–HDEHP–CMPO system were analyzed using HypSpec spectral analysis software. For this data treatment, it was assumed that Nd(DEHP)$_3$ existed as a single entity in solution and that there was no dissociation of the DEHP$^-$ anion in the nonpolar *n*-dodecane diluent. The Nd(III)–HDEHP–CMPO FTIR data was best fit by considering the equilibrium:

$$\text{Ln(DEHP)}_3 + \text{CMPO} \rightleftharpoons \left[\text{Ln(CMPO)(DEHP)}_3 \right], \tag{11}$$

where Ln = Nd. Table 3 presents the log K values for equilibrium (11) determined both by the FTIR and the Vis spectroscopic data. The log K values determined using HypSpec are considered to be conditional, since no account has been made for solution nonideality. The K values determined by the two spectral methods differ somewhat, with that determined by spectrophotometry being approximately 2.5 times higher than that determined by FTIR. The value obtained spectrophotometrically is probably more reliable since there are fewer spectral interferences in that data set with Nd(DEHP)$_3$ and [Nd(CMPO)(DEHP)$_3$] being the only absorbing species in the spectral range 550–620 nm (figure 4).

In the case of the Eu(III)/HDEHP/CMPO system, the Eu(III) concentration in the fully loaded organic phase was 0.0524 mol L^{-1} and the total HDEHP concentration was 0.3021 mol L^{-1}. Assuming the complex stoichiometry to be Eu(DEHP)$_3$, 48% of the HDEHP remained uncomplexed in the loaded solvent (0.145 mol L^{-1} uncomplexed HDEHP), a value much higher than observed for the analogous Nd system. Figure S1(a) (Supplementary material) illustrates the changes in the ν(C=O) region of the FTIR spectrum for selected conditions upon addition of CMPO to the Eu(DEHP)$_3$ solution. Similar to what was observed for Nd(III), two bands become evident in the ν(C=O) region as CMPO is added to the Eu(DEHP)$_3$ solution. The band at 1637 cm^{-1} is assigned to the CMPO·HDEHP adduct. The other band, located at 1601 cm^{-1}, is attributed to the Eu(DEHP)$_3$·CMPO complex.

Figure S1(b) shows the phosphorus–oxygen stretching region in the FTIR spectrum for the Eu(III)/HDEHP/CMPO system. Upon loading with Eu(III), the HDEHP ν(P=O) band shifts from 1231 to 1203 cm^{-1}, a result very similar to that obtained with Nd(III). Addition of CMPO to the Eu(DEHP)$_3$ complex slightly shifts the ν(P=O) band to 1207 cm^{-1}, providing further evidence for binding of CMPO to the Eu(III) center. Again, bands associated with the CMPO·HDEHP adduct (e.g., 1263 and 1000 cm^{-1}) become increasingly evident as the CMPO concentration is increased in the Eu(DEHP)$_3$ solution.

Table 3 presents the $\log K$ value for complexation (equation (11)) of Eu(III) by CMPO. The results indicated that complexation of CMPO to Eu(DEHP)$_3$ is weaker than that to Nd(DEHP)$_3$, the difference in the $\log K$ value being approximately 1.6. This is consistent with the results of the SXLSQI modeling of the liquid–liquid extraction data, which also indicated stronger complexation of CMPO to Nd(III) *versus* Eu(III) (*vide supra*). The stronger complexation of CMPO to Nd(III) might be due to greater steric crowding around the smaller Eu(III) ion compared to Nd(III). Alternatively, the stronger complexation of the DEHP$^-$ ion to Eu(III) might reduce the acidity of Eu(III) relative to Nd(III) by contributing greater electron density to the Eu(III) metal center. Application of theoretical techniques might help to distinguish between these two possible explanations.

4. Discussion

Owing to the high coordination numbers available to the trivalent lanthanide and actinide ions (CN 8 to 10), formation of ternary complexes is not a rare phenomenon for these ions. Ternary complexes of the *f*-block elements with aminopolycarboxylates is particularly well-documented and has recently been reviewed [30]. In the context of lipophilic ternary *f*-block element complexes, experimental and theoretical studies of lanthanide complexes containing 4,4,4-trifluoro-1(2-thienyl)-1,3-butanedione and tri-*n*-butylphosphate ligands have been recently described [31, 32]. Relevant to the work described here are ternary complexes containing CMPO. Indeed, the key mechanism for extracting the trivalent lanthanides and actinides from nitric acid media in the TRUEX process involves the formation of lipophilic M(III)–CMPO–nitrate ternary species [33]:

$$M^{3+}(aq) + 3NO_3^-(aq) + 3CMPO(org) \rightleftharpoons \left[M(NO_3)_3(CMPO)_3\right](org). \qquad (12)$$
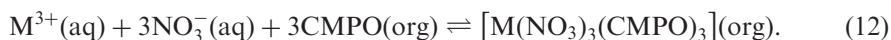
Thus, there is precedent for the formation of ternary species containing the CMPO ligand. On the other hand, there is little evidence for the formation of ternary complexes in the TALSPEAK process chemistry involving the HDEHP extractant. Although ternary M(III)–HDEHP–lactate species were hypothesized to form in the TALSPEAK extraction system [23], a meticulous search for such species found no evidence for them [34].

In this work, the formation of ternary Ln–DEHP–CMPO complexes has been explored through application of liquid–liquid extraction and spectroscopic techniques. Both methods reveal the formation of such ternary complexes. The precise nature of the species formed is not known, but the FTIR spectra strongly suggest that the CMPO ligand is coordinated in bidentate fashion though the carbonyl and phosphoryl oxygen atoms. Figure 5 presents a speculative illustration of the ternary complex, [Ln(CMPO)(AHA)$_2$(A)], formed under conditions of the liquid–liquid extraction experiments described in this article. It is hypothesized that such a complex would contain a bidentate CMPO ligand and two bidentate AHA$^-$ ligands. The latter ligand consists of two individual DEHP anions held together *via* a hydrogen bond, forming a bidentate ligand that binds through the phosphoryl oxygen atoms of the DEHP moiety. Finally, an A$^-$ ion binds the metal center in either a monodentate or bidentate fashion (the bidentate mode is illustrated in figure 5). Monodentate coordination of the A$^-$
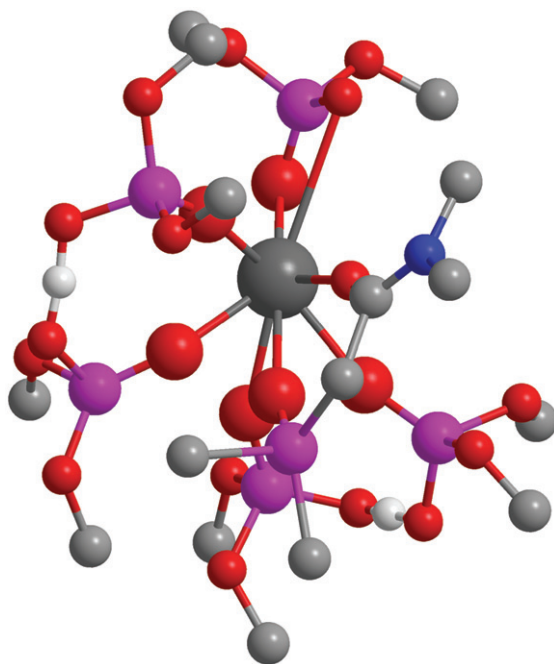
G.J. Lumetta et al.

Figure 5. Illustration of hypothetical structure of a [Ln(CMPO)(AHA)$_2$(A)] complex. For clarity, the various substituents on the CMPO and HDEHP ligands have been replaced with methyl groups, and the hydrogen atoms on the alkyl groups are not shown.

ligand would lead to a coordination number of 7 whereas the bidentate mode would lead to coordination number 8; the latter situation is considered more likely.

The role of ternary complexes of *f*-block elements in the process chemistry of liquid–liquid separations schemes is not fully understood, and further investigation of such systems is warranted. The formation of such species in both the aqueous phase and the organic phase might be important to the overall performance of the desired separation. Understanding the role of ligand electronic and molecular structure in the propensity to form ternary complexes with the lanthanides and actinides could lead to design of new highly efficient processes for intragroup and intergroup separations of the lanthanides and actinides.

Acknowledgments

References

[1] T.V. Smith. *J. Inorg. Nucl. Chem.*, **19**, 314 (1961).
[2] W.J. McDowell, G.N. Case, D.W. Aldrup. *Sep. Sci. Technol.*, **18**, 1483 (1983).
[3] V.V. Rublev. *J. Anal. Chem. USSR*, **38**, 707 (1983).

[4] V.V. Ramakrishna, S.K. Patil. *Struct. Bond.*, **56**, 35 (1984).
[5] IUPAC (Ed.). *Compendium of Chemical Terminology*, 2nd Edn, Blackwell Scientific Publications, Oxford (1997). XML on-line corrected version: http://goldbook.iupac.org (2006) created by M. Nic, J. Jirat, B. Kosata; updates compiled by A. Jenkins. ISBN 0-9678550-9-8. doi:10.1351/goldbook (accessed 03 January 2012).
[6] G.J. Lumetta, A.V. Gelis, G.F. Vandegrift. *Solvent Extr. Ion Exch.*, **29**, 287 (2010).
[7] P.S. Dhami, R.R. Chitnis, V. Gopalakrishnan, P.K. Wattal, A. Ramanujam, A.K. Bauri. *Sep. Sci. Technol.*, **36**, 325 (2001).
[8] G.J. Lumetta, J.C. Carter, A.V. Gelis, G.F. Vandegrift. In *Nuclear Energy and the Environment*, C.M. Wai, B.J. Mincher (Eds), pp. 107–118, American Chemical Society, Washington, DC (2010).
[9] E.P. Horwitz, D.G. Kalina, H. Diamond, G.F. Vandegrift, W.W. Schulz. *Solvent Extr. Ion Exch.*, **3**, 75 (1985).
[10] B. Weaver, F.A. Kappelmann. *J. Inorg. Nucl. Chem.*, **30**, 263 (1968).
[11] J.A. Partridge, R.C. Jensen. *J. Inorg. Nucl. Chem.*, **31**, 2587 (1969).
[12] P.D. Watson. *Ind. Eng. Chem.*, **32**, 399 (1940).
[13] C.F. Baes Jr. *SXLSQI: A Program for Modeling Solvent Extraction Systems, ORNL/TM-13604*, Oak Ridge National Laboratory, Oak Ridge, Tennessee (1998).
[14] K.S. Pitzer. In *Activity Coefficients in Electrolyte Solutions*, K.S. Pitzer (Ed.), 2nd Edn, pp. 75–153, CRC Press, Boca Raton, FL (1991).
[15] A.F.M. Barton. *CRC Handbook of Solubility Parameters and Other Cohesion Parameters*, CRC Press, Boca Raton, FL (1991).
[16] F.J. Millero. In *Structure and Transport Processes in Water and Aqueous Solutions*, R.A. Horne (Ed.), pp. 519–595, Wiley & Sons, New York (1972).
[17] C. Scharf, A. Ditze, K. Schwerdtfeger, S. Fürmeier, T. Bruhn, D.E. Kaufmann, J.C. Namyslo. *Metall. Mater. Trans. B*, **36B**, 429 (2005).
[18] P. Gans, A. Sabatini, A. Vacca. *Talanta*, **43**, 1739 (1996).
[19] R. Lundqvist, J.-F. Lu, I. Svantesson. *Acta Chem. Scand.*, **A37**, 743 (1983).
[20] D.F. Peppard, G.W. Mason, W.J. Driscoll, R.J. Sironen. *J. Inorg. Nucl. Chem.*, **7**, 276 (1958).
[21] D.F. Peppard, G.W. Mason, J.L. Maier, W.J. Driscoll. *J. Inorg. Nucl. Chem.*, **4**, 344 (1957).
[22] J.M. Sánchez, M. Hidalgo, V. Salvadó, M. Valiente. *Solvent Extr. Ion Exch.*, **17**, 455 (1999).
[23] M. Nilsson, K.L. Nash. *Solvent Extr. Ion Exch.*, **25**, 665 (2007).
[24] M. Zangen. *J. Inorg. Nucl. Chem.*, **28**, 1693 (1966).
[25] P. Gen, X. Wang. *Beijing Daxue Xuebao Ziran Kexueban*, **5**, 59 (1982).
[26] G.J. Lumetta, D. Neiner, S.I. Sinkov, J.C. Carter, J.C. Braley, S.L. Latesky, A.V. Gelis, G.F. Vandegrift. Combining neutral and acidic extractants for recovering transuranic elements from nuclear fuel. In *Proceedings of the 19th International Solvent Extraction Conference*, Gecamin Ltd, Santiago, Chile, Paper No. 68 (2011).
[27] T.G. Levitskaia. *Non-Ideality in Solvent Extraction Systems: PNNL FY 2011 Status Report, PNNL-20662*, Pacific Northwest National Laboratory, Richland, WA (2011).
[28] K. Bukietynska, A. Mondry, E. Osmeda. *J. Inorg. Nucl. Chem.*, **43**, 1321 (1981).
[29] G.R. Choppin, J.A. Chopoorian. *J. Inorg. Nucl. Chem.*, **22**, 97 (1961).
[30] G.R. Choppin, P. Thakur, J.N. Mathur. *Coord. Chem. Rev.*, **250**, 936 (2006).
[31] Z. Szabó, V. Vallet, I. Grenthe. *Dalton Trans.*, **39**, 10944 (2010).
[32] V. Vallet, Z. Szabó, I. Grenthe. *Dalton Trans.*, **40**, 3154 (2011).
[33] E.P. Horwitz, H. Diamond, K.A. Martin, R. Chiarizia. *Solvent Extr. Ion Exch.*, **5**, 419 (1987).
[34] C.J. Leggett, G. Liu, M.P. Jensen. *Solvent Extr. Ion Exch.*, **28**, 313 (2010).